Dislocation densities reduction in MBE-grown AlN thin films by high-temperature annealing

Maud Nemoz, Roy Dagher, Samuel Matta, Adrien Michon, Philippe Vennégues, Julien Brault

▶ To cite this version:

Maud Nemoz, Roy Dagher, Samuel Matta, Adrien Michon, Philippe Vennégues, et al.. Dislocation densities reduction in MBE-grown AlN thin films by high-temperature annealing. Journal of Crystal Growth, Elsevier, 2017, 461, pp.10-15. 10.1016/j.jcrysgro.2016.12.089 . hal-03543886

HAL Id: hal-03543886

https://hal-cnrs.archives-ouvertes.fr/hal-03543886

Submitted on 26 Jan 2022

HAL is a multi-disciplinary open access archive for the deposit and dissemination of scientific research documents, whether they are published or not. The documents may come from teaching and research institutions in France or abroad, or from public or private research centers.

L'archive ouverte pluridisciplinaire **HAL**, est destinée au dépôt et à la diffusion de documents scientifiques de niveau recherche, publiés ou non, émanant des établissements d'enseignement et de recherche français ou étrangers, des laboratoires publics ou privés.

Dislocation densities reduction in MBE-grown AlN thin films by high-temperature annealing

Maud Nemoz[1], Roy Dagher[1,2], Samuel Matta[1,3], Adrien Michon[1], Philippe Vennéguès[1], and Julien Brault[1]

[1]*CNRS-CRHEA, Rue B. Gregory, 06560 Valbonne, France*

[2]*Université de Nice Sophia-Antipolis, 06103 Nice, France*

[3]*L2C, UMR 5221, Case courrier 074-34095 Montpellier Cedex 5, France*

ABSTRACT

AlN thin films, grown on (0001) sapphire substrates by molecular beam epitaxy (MBE), were annealed at high temperature (up to 1650 °C) in flowing N_2. X-ray diffraction (XRD) studies, combined with Williamson-Hall and Srikant plots, have shown that annealing leads to a strong reduction of both edge and mixed threading dislocation densities, as confirmed by transmission electron microscopy (TEM) images, up to 75%. Moreover, it is found that annealing at high temperatures allows the relaxation of the tensile strain in the AlN film due to the growth process. In addition, the morphological properties of the films were determined by atomic force microscopy (AFM) and show that the annealing conditions have a strong impact on the surface morphology and roughness. Finally, an annealing at 1550 °C for 20 minutes appears as an ideal tradeoff to enhance the structural properties while preserving the initial AlN surface morphology.

I. INTRODUCTION

Aluminum nitride has generated much interest for applications in the deep-ultraviolet region because of its wide direct band gap and high chemical and thermal stabilities.[1,2] The most commonly used substrate for AlN growth is sapphire due to its relatively low cost. However, high-density of threading dislocations (TD) usually exist in AlN epitaxial films owing to important differences (chemistry, structure, lattice parameters) between AlN and sapphire. Most of TD lines in AlN epitaxial films are normal to the substrate and form the boundaries of sub-grains. More precisely, three main types of TDs are observed: pure screw (c-type, Burger vector = <0001>), pure edge (a-type, Burger vector = 1/3<11-20>) and mixed ((a+c)-type, Burger vector = 1/3<11-23>). In nitride materials, pure edge dislocations and mixed TD are known to be prominent, while pure screw dislocations represent a very small proportion (~1%) of all TDs.[3-5] Therefore, in this study, we will only investigate and take into account edge and mixed TD densities (TDDs).

There have been several approaches to reduce these defects, one of the most promising one being the post-growth annealing. Since the last decade, the annealing of the AlN films have been studied on films grown by sputtering,[6] pulsed laser deposition (PLD)[7], metal-organic vapor phase epitaxy (MOVPE)[8,9] and molecular beam epitaxy (MBE).[10-12] In particular, the AlN films grown by MBE on sapphire substrates have been annealed under N_2 atmosphere at various temperatures and durations, from multiple cycles of 10 s, up to 1200 °C,[11] to recently a combination of a 30 min annealing at 1150 °C followed by 20 pulses up to 1520 °C.[12] This last work reports a good enhancement of the ω-scan full width at half maximum (FWHM) for the 0002 symmetric reflection (70%) but much less enhancement for the 10-12 skew symmetric one (14%). In the present study, we use some microstructural models to link the ω-scan FWHMs to the TDDs in our samples and confirm the validity of the models by comparing the results with the TDDs determined from transmission electron microscopy (TEM) measurements. We report a reduction as high as 75% for both mixed and edge TDDs with a simple annealing process at high temperature, indicating its efficiency to strongly improve the AlN epitaxial layer structural quality.

II. EXPERIMENTAL PROCEDURE

The AlN thin films were grown on (0001) sapphire substrates by molecular beam epitaxy (MBE) in a RIBER 32 P reactor. Solid sources were used for the III-elements and ammonia (NH_3) was employed as the nitrogen precursor. Two samples were initially fabricated. For the sample S1 (resp. S2) a 10 min nitridation step at 940 °C (resp. 900 °C), was followed by the deposition of one monolayer of Al at 400 °C and the growth of a 5 nm thick AlN buffer layer at 450°C. Then, a 120 nm thick AlN layer has been deposited at 940°C (resp. 900 °C) at a growth rate of about 70 nm/h and a V/III ratio of 70. For both samples, the RHEED pattern indicated a (1x1) surface reconstruction during growth, but during the cooling down process under NH_3, a transition from (1x1) to (2x2) was observed for temperatures below 550°C, which indicates an Al polarity of the layers. The two initial as-grown samples were then cleaved to form the S1 and S2 samples series, referring to the growth temperature of 940 °C and 900 °C for the AlN layer, respectively.

For the annealing, we used a horizontal hot wall chemical vapor deposition reactor. The annealing was conducted at temperatures ranging from 1350 to 1650 °C under a constant laminar flow of 6 slm (standard litres per minute) of N_2 with a pressure of 0.8 bars. The temperature was monitored using a pyrometer focused on the substrate holder just beneath the sample. After the temperature ramp up, the sample was left under the carrier gas for a 5 minute-plateau, then the heating was cut off, and the sample left under the carrier gas for cooling down to room temperature. The S1 samples series has been annealed at 1350, 1550 and 1650 °C, and the S2 samples series has been annealed at 1350, 1450, 1550 and 1650 °C. The effect of the annealing duration has also been studied with three additional samples from the S2 series, all of them annealed at 1550 °C. For the first one, only a ramp of temperature has been done (no plateau), that is to say, an increase of temperature until 1550 °C followed by an immediate decrease of temperature. For the second sample, 3 successive ramps of temperature, from room temperature to 1550 °C and back to room temperature, have been done. The third sample has been annealed a first time for 5 min and a second time for 15 min.

X-ray diffraction has been performed with a PANalytical X'Pert PRO MRD four-circle diffractometer. The dislocation densities of the AlN films have been determined from symmetric and skew symmetric ω-scans recorded in the open detector configuration. Regarding the *c* lattice parameter, it has been determined from 2θ-ω scans measured with an analyzer crystal before the detector. Atomic force microscopy images have been recorded with a Bruker Dimension 3100 in Tapping Mode, and images have been processed using WSxM software.[13] Some of the samples have been studied by transmission electron microscopy (TEM) in plan-view orientation in order to quantitatively determine the TD densities. TEM specimens have been prepared by wedge polishing. The observations have been conducted using a JEOL 2100F field emission TEM.

III. RESULTS AND DISCUSSION

Figure 1 shows the ω-scan full width at half maximum (FWHM) of the 0002 symmetric reflection (a) and the 10-11 skew symmetric reflection (b) as a function of the annealing temperature for the two series of samples. The dots corresponding to the as-grown samples in the figure are placed at the AlN growth temperatures. As a general trend, for both the 0002 and the 10-11 reflections, the ω-scan FWHM decreases when the annealing temperature increases, indicating an improvement in the structural quality of the AlN film. When the annealing duration increases, the ω-scan FWHM also decreases for both reflections: we observe that the 1-ramp annealing at 1550 °C is less efficient that the 5 min annealing at 1550 °C, and even less efficient than the 5 min annealing at 1450 °C. Yet, the 3-ramps annealing seems to be slightly better than the 5 min annealing at 1450 °C. Finally the 2 step annealing (5 min and 15 min) at 1550 °C seems to have almost the same effect that the 5 min annealing at 1650 °C. Therefore, the improvement of the grain size by atomic rearrangement in the AlN films is also strongly time-dependent, with an asymptotical behavior, i.e. with a stronger influence during the first minutes of the process.

Nitride epitaxial films grown on sapphire are often described as crystals with a mosaic structure that can be characterized by means of tilt and twist angles. The tilt angle represents the out-of-plane rotation of the mosaic blocks, while the twist angle describes their in-plane rotation. The ω-scans FWHM is

influenced by several factors such as the instrumental width, the lattice rotations due to dislocations (tilt and twist), the lattice strain, the coherence length and the wafer curvature. However, for relatively high dislocation density films, the tilt and twist broadening dominates[14,15] and can be used as a measure of the dislocation densities. The symmetric reflections are affected by the out-of-plane lattice rotation whereas the skew symmetric reflections are sensitive to both the out-of-plane and the in-plane lattice rotation. Hence, tilt and twist can be determined from the symmetric and skew symmetric reflections through Williamson-Hall plot and Srikant plot, respectively. Figure 2 (a) shows the Williamson-Hall plot[16] for the S2 series, where the slope of the straight line fit corresponds to the tilt value of each sample. ω-scans have been measured in open detector configuration for three symmetric reflections: 0002, 0004 and 0006. Then, the integral breadth β (i.e. the ratio of the peak area over the peak maximum intensity) has been used to take into account the shape of the ω-scan peak for the symmetric reflections. Indeed, for a Gaussian peak, β is similar to the FWHM, but for a Lorentzian peak, β is equal to 0.62 times the FWHM.[17] Figure 2 (b) shows the ω-scan FWHM for the S2 series as a function of χ, the angle between the diffracting plane and the (0002) growth plane. The 30-32 reflection (corresponding to the maximum value of χ) and the 10l reflections for l=1 to 5 (corresponding to the other values of χ, which are decreasing for increasing values of l) have been measured. Both the tilt and the twist values influence the ω-scan FWHM of a skew symmetric reflection. The solid lines correspond to the fit of the measured FWHM with the Srikant's model[18] to determine the twist value of each sample:

$$FWHM_{fit} = (FWHM_{tilt}{}^{n} + FWHM_{twist}{}^{n})^{1/n}, \quad (1)$$

$$\text{with } FWHM_{tilt} = cos^{-1}[cos^{2}(\chi)\cos(tilt) + sin^{2}(\chi)], \quad (2)$$

$$\text{and } FWHM_{twist} = cos^{-1}[sin^{2}(\chi)\cos(twist) + cos^{2}(\chi)], \quad (3)$$

n depending on the peak shape (here $1.5<n<2$).

The ordinate at origin corresponds to the tilt value determined with the Williamson-Hall plot. The tilt and twist values determined from Williamson-Hall plot and Srikant plot are presented in Table I. Both tilt and twist values decrease when the annealing temperature increases, indicating an improvement of

the microstructure quality of the AlN film. For the S2 series, the tilt and twist values have been reduced by about 50 % after the 5 min annealing at 1650 °C.

TABLE. I. Tilt and twist values for the two series of samples.

Sample	**S1 tilt (°)**	**S2 tilt (°)**	**S1 twist (°)**	**S2 twist(°)**
As-grown	0.73	0.93	1.20	1.60
1350	0.68	0.80	1.15	1.52
1450	-	0.63	-	1.22
1550	0.44	0.49	0.78	0.96
1650	0.50	0.45	0.58	0.78

A lot of models have been proposed to calculate the dislocation densities from the thin films tilt and twist values, assuming a mosaic structure[19-21] or a random distribution of dislocations.[22,23] For high dislocation densities, the difference between the results obtained assuming one or the other hypothesis is small.[20,21] The screw (resp. edge) dislocations, with a Burger vector *c* = <0001> (resp. a = 1/3<11-20>), influence the tilt (resp. twist) value of the thin films. The mixed dislocations (Burger vector a+c = 1/3<11-23>) influence both the tilt and the twist values. In this paper, we will distinguish only edge and mixed TDs because the screw TDs represent a very low proportion (~1%) of all TDs in nitride materials.[5] The edge threading dislocation densities have been determined with the equation proposed by Dunn and Koch:[22]

$$\rho = \frac{\alpha^2}{4.35\times b^2}\ , \qquad (4)$$

where b is the burger vector of the edge dislocation and α is the twist value. Assuming that the tilt is only due to mixed TDs (due to the very low proportion of pure screw dislocations) mixed TDDs can be calculated from the tilt using the same formula. Figure 3 shows the calculated mixed TDDs (a) and the calculated edge TDDs (b) versus the annealing temperature. The mixed and the edge TDDs decrease with increasing annealing temperature. For the S2 series, the mixed TDDs have been reduced by 77% and the edge TDDs have been reduced by 76%. The TDDs calculated from XRD measurements and

with the Dunn and Koch equation are in good agreement with the TDDs determined from transmission electron microscopy (TEM) measurements: for the S1 sample series, a TDD of about 3.10^{11} cm^{-2} (resp. 1.10^{11} cm^{-2}) has been measured from TEM plane view images (resp. XRD measurements) before annealing and a TDD of 2.10^{10} cm^{-2} (resp. 4.10^{10} cm^{-2}) after the 5 min annealing at 1550 °C (Figure 4). It is noticeable on Figure 3 that there is a critical temperature for the TDD reduction. Below 1350°C, the TDD reduction is low whereas it becomes more efficient above that temperature. TDD reduction mechanism involves a movement of the TDs. In fact, moving TDs may interact and annihilate. TDs move by glide or climb processes. Vertical a and (a+c)-dislocations may only glide in prismatic {10-10} planes. On one hand, it can be assumed that the weak reduction of TDDs below 1350°C is related to such a glide process. On the other hand, the TDD reduction above 1350°C may be ascribed to climb processes thanks to the introduction of vacancies and easier atomic rearrangements at such high temperatures.

Figure 5 (a) shows (5 x 5 μm^2) AFM images illustrating the evolution of the AlN surface morphology with the annealing temperature for the S2 sample series. Some aggregates (white spots) are present on the surface of the as-grown sample while no pits are observed. After the 1350 °C and 1450°C annealing, some aggregates are still present and pits appear. After the 1550 °C annealing, the pits seem to become larger and finally after the 1650 °C annealing, numerous aggregates are present and larger pits can be seen, probably due to the decomposition of AlN above 1400 °C.[10] Figure 5 (b) shows the variation of the AlN surface Root Mean Square (RMS) roughness, determined from the AFM images, with the annealing temperature for the two sample series. The RMS of the two as-grown samples is typically around 1 nm. After the annealing at 1350 and 1450°C, the RMS is decreased, whereas after the annealing at 1550 °C the RMS is slightly increased. The numerous aggregates and pits present after the 1650 °C annealing provoke a strong increase of the RMS. The variation of the annealing duration at 1550 °C indicates that the surface degradation increases with the annealing duration: considering samples annealed at 1550°C, the lowest RMS is obtained for the 1-ramp process while the highest RMS is obtained for the 2 step (5 and 15 min) process. Taking into account the roughening of the surface along with the improvement of the microstructure, we can determine that a long (5+15 min) annealing

at 1550 °C enables us to improve the microstructure as much as a short (5 min) annealing at 1650 °C but with much less damaging of the surface. Therefore, this long annealing process at an intermediate temperature seems to be the best compromise compared to a shorter annealing process at higher temperature.

The epitaxial thin films generally undergo in-plane stress due to lattice mismatch and thermal expansion coefficient (TEC) mismatch between the film and the substrate. Assuming that there is no plastic relaxation during the cooling down to room temperature (no dislocation introduction or suppression), two situations may be considered: on one hand, if during the growth the film has a perfect epitaxial relation with the substrate, then the in-plane lattice parameter of the layer will be that of the substrate and does not depend on the growth temperature. Therefore only the lattice mismatch (LM) between the layer and the substrate at room temperature has to be taken into account to determine the final strain in AlN:

$$\varepsilon_a = \varepsilon_a^{LM} = (a_s - a_f)/a_f, \tag{5}$$

where a_f and a_s are respectively the in-plane lattice parameters of the film and the substrate.

On the other hand, if during the high temperature growth, the layer is fully relaxed, then only the TEC mismatch would be involved in the final strain state of AlN at room temperature, with the equation:

$$\varepsilon_a = \varepsilon_a^{TEC} = (\alpha_f - \alpha_s)\Delta T, \tag{6}$$

where α_f and α_s are respectively the TEC of the film and the substrate, and ΔT is difference between the growth temperature and the room temperature.

Consequently, in a general way, the final film strain value should be comprised between that being due to the lattice mismatch and that resulting from the TEC mismatch between AlN and sapphire. However, when the epitaxial growth includes the coalescence of 3D islands to form the epitaxial layer, which is the case for AlN on sapphire, the tensile stress generated by the coalescence of 3D islands[24,25] can lead to a remaining tensile strain at room temperature. Thus, including the additional coalescence tensile strain (ACTS), the final strain of the AlN layer should be in the range of:

$$\varepsilon_a^{LM} + \Delta\varepsilon_a^{ACTS} < \varepsilon_a < \varepsilon_a^{TEC} + \Delta\varepsilon_a^{ACTS}. \quad (7)$$

For the AlN films grown on sapphire, on one hand, the lattice mismatch (for the 8:9 ratio of Al-Al distances[26]) should lead to a compressive strain ε_a^{LM} of about -0.7%, and on the other hand, the TEC mismatch[27] should result in a compressive strain ε_a^{TEC} up to -0.3% for a growth temperature of 940 °C. Nevertheless, both S1 and S2 as-grown samples have shown a tensile strain ε_a of about 0.2% indicating that the tensile stress generated during grain coalescence dominates the epitaxial and thermal stress in these thin films. Therefore, the additional coalescence tensile strain $\Delta\varepsilon_a^{ACTS}$ can be estimated in the range between (i) the difference between the measured strain ε_a and the TEC mismatch strain ε_a^{TEC}, and (ii) the difference between the measured strain ε_a and the lattice mismatch strain ε_a^{LM}, i.e. between (i) 0.5% and (ii) 0.9%. The in-plane strain ε_a has been determined from the out-of-plane strain ε_c of the AlN films with the equations:

$$\varepsilon_a = -\frac{C_{33}}{2C_{13}}\varepsilon_c \,, \quad (8)$$

$$\text{and } \varepsilon_c = \frac{c_{film} - c_{bulk}}{c_{bulk}} \,, \quad (9)$$

where the elastic constant values C_{33} and C_{13} are those determined by Wright *et al* .[28] The c_{bulk} value of AlN used is 4.982 Å[29] and the c_{film} has been calculated from the 2θ-ω scan of the 0002 symmetric reflection recorded with an analyzer crystal before the detector.

Figure 6 shows the in-plane strain ε_a of the AlN layers vs. the annealing temperature. The blue and red dashed horizontal lines correspond to the as-grown strain of about 0.2%. The black horizontal dot line corresponds to the theoretical lattice mismatch of -0.7% and the black straight line corresponds to the theoretical TEC strain varying between -0.4% and -0.6% in the annealing temperature range. For both series of samples, the initial tensile strain decreases with annealing temperature to become a compressive strain after the annealing above 1450 °C. The relation between the strain variation and the TDD reduction is not obvious. Firstly, most of TDs are aligned perpendicular to the film-substrate interface and cannot relieve the in-plane stress effectively. Secondly, misfit dislocations may only be introduced by glide in inclined pyramidal planes. This kind of glide process is unlikely because it

involves (a+c)-type dislocations which have a large Burger vector and therefore large nucleation energy. Strain relaxation therefore requires climb processes for either introduction of new misfit dislocations or reorientation of preexisting TDs. Consequently, the strain evolution with the annealing temperature in these AlN layers is consistent with the TDD reduction as shown in Fig. 3. It is again noticeable that the strain relaxation is only efficient for temperature above 1350°C. It appears that this temperature is critical for any process requiring dislocation movement, TDD reduction or strain relaxation. Finally, these dislocation motions enable to reduce the coalescence tensile strain, initially comprised in the range of 0.5-0.9%, to the range of 0.3-0.5% after the annealing at 1650 °C.

IV. CONCLUSION

Two series of AlN epitaxial layers have been grown at 900 and 940 °C on (0001) sapphire substrates by molecular beam epitaxy. The effect of high temperature annealing has been studied on both series of samples with post-growth annealing carried out from 1350 to 1650 °C for different durations in flowing N_2. For the 0002 and the 10-11 reflections, the ω-scan FWHM decreases when the annealing temperature increases, which indicates an improvement in the structural quality of the AlN layer. This improvement is found to be almost the same between a 5 min annealing at 1650 °C and a 2 step annealing (5 and 15 min) at 1550 °C. Tilt values of the AlN films have been determined from the Williamson-Hall plot of the 000l symmetric reflections. Twist values have been determined from Srikant model of the h0-hl skew symmetric reflections. Then, mixed (resp. edge) threading dislocation densities have been evaluated from tilt (resp. twist) values. For the 5 min annealing at 1650 °C, both mixed and edge TDDs decrease in almost the same percentage of 75%. The strain evolution of the AlN layers with the annealing temperature is consistent with the TDD reduction and shows that the annihilation of some TDs enables to reduce the additional coalescence tensile strain coming from the coalescence of 3D islands to form the epitaxial layer. The surface roughness (RMS) of the AlN films has been determined by AFM and shows a dramatic increase after the annealing at 1650 °C. Finally, the analysis of the structural

enhancement and the surface roughening with annealing temperature and duration seems to indicate a best compromise for the annealing at 1550 °C for 20 min.

ACKNOWLEDGEMENTS

P.V. wants to thank IMRA Europe S.A. for the access to the STEM JEOL 2100 microscope. This work had been supported in part by the "Agence Nationale de la Recherche" within the "NANOGANUV" Project No. ANR-14-CE26-0025-01.

REFERENCES

[1] Y. Taniyasu, M. Kasu, and T. Makimoto, Nature **441**, 325 (2006).

[2] N. Faleev, H. Lu, and W.J. Schaff, J. Appl. Phys. **101**, 093516 (2007).

[3] W. Gian, M. Skowronski, and G.S. Rohrer, in *MRS Proc.* (Cambridge Univ Press, 1996), p. 475.

[4] S.R. Lee, A.M. West, A.A. Allerman, K.E. Waldrip, D.M. Follstaedt, P.P. Provencio, D.D. Koleske, and C.R. Abernathy, Appl. Phys. Lett. **86**, 241904 (2005).

[5] M.A. Moram, C.S. Ghedia, D.V.S. Rao, J.S. Barnard, Y. Zhang, M.J. Kappers, and C.J. Humphreys, J. Appl. Phys. **106**, 073513 (2009).

[6] J.P. Kar, G. Bose, and S. Tuli, Mater. Sci. Semicond. Process. **8**, 646 (2005).

[7] K.A. Jones, M.A. Derenge, T.S. Zheleva, K.W. Kirchner, M.H. Ervin, M.C. Wood, R.D. Vispute, R.P. Sharma, and T. Venkatesan, J. Electron. Mater. **29**, 262 (2000).

[8] W.-Y. Wang, P. Jin, G.-P. Liu, W. Li, B. Liu, X.-F. Liu, and Z.-G. Wang, Chin. Phys. B **23**, 087810 (2014).

[9] H. Miyake, G. Nishio, S. Suzuki, K. Hiramatsu, H. Fukuyama, J. Kaur, and N. Kuwano, Appl. Phys. Express **9**, 025501 (2016).

[10] Z.Y. Fan, G. Rong, N. Newman, and D.J. Smith, Appl. Phys. Lett. **76**, 1839 (2000).

[11] J.D. Greenlee, B. Gunning, B.N. Feigelson, T.J. Anderson, A.D. Koehler, K.D. Hobart, F.J. Kub, and W.A. Doolittle, Electron. Mater. Lett. **12**, 133 (2016).

[12] B. Liu, J. Gao, K.M. Wu, and C. Liu, Solid State Commun. **149**, 715 (2009).

[13] I. Horcas, R. Fernández, J.M. Gómez-Rodríguez, J. Colchero, J. Gómez-Herrero, and A.M. Baro, Rev. Sci. Instrum. **78**, 013705 (2007).

[14] T.A. Lafford, B.K. Tanner, and P.J. Parbrook, J. Phys. Appl. Phys. **36**, A245 (2003).

[15] M.E. Vickers, M.J. Kappers, R. Datta, C. McAleese, T.M. Smeeton, F.D.G. Rayment, and C.J. Humphreys, J. Phys. Appl. Phys. **38**, A99 (2005).

[16] G.K. Williamson and W.H. Hall, Acta Met. **1**, 22 (1953).

[17] M.A. Moram and M.E. Vickers, Rep. Prog. Phys. **72**, 036502 (2009).

[18] V. Srikant, J.S. Speck, and D.R. Clarke, J. Appl. Phys. **82**, 4286 (1997).

[19] P. Gay, P.B. Hirsch, and A. Kelly, Acta Met. **1**, 315 (1953).

[20] T. Metzger, R. Höpler, E. Born, O. Ambacher, M. Stutzmann, R. Stömmer, M. Schuster, H. Göbel, S. Christiansen, M. Albrecht, and H.P. Strunk, Philos. Mag. A **77**, 1013 (1998).

[21] R. Chierchia, T. Böttcher, H. Heinke, S. Einfeldt, S. Figge, and D. Hommel, J. Appl. Phys. **93**, 8918 (2003).

[22] C.G. Dunn and E.F. Koch, Acta Met. **5**, 548 (1957).

[23] V.M. Kaganer, O. Brandt, A. Trampert, and K.H. Ploog, Phys. Rev. B **72**, (2005).

[24] D. Magnfält, Dissertations. No. 1592, Department of Physics, Chemistry and Biology (IFM), Linköping University, 2014.

[25] S. Raghavan and J.M. Redwing, J. Appl. Phys. **96**, 2995 (2004).

[26] C.J. Sun, P. Kung, A. Saxler, H. Ohsato, K. Haritos, and M. Razeghi, J. Appl. Phys. **75**, 3964 (1994).

[27] H. Morkoç, S. Strite, G.B. Gao, M.E. Lin, B. Sverdlov, and M. Burns, J. Appl. Phys. **76**, 1363 (1994).

[28] A.F. Wright, J. Appl. Phys. **82**, 2833 (1997).

[29] Y. Goldberg, in *Properties of advanced semiconductor materials*, edited by M. E. Levinshtein, S. L. Rumyantsev, M. S. Shur (Wiley, New York, 2001).

FIGURES

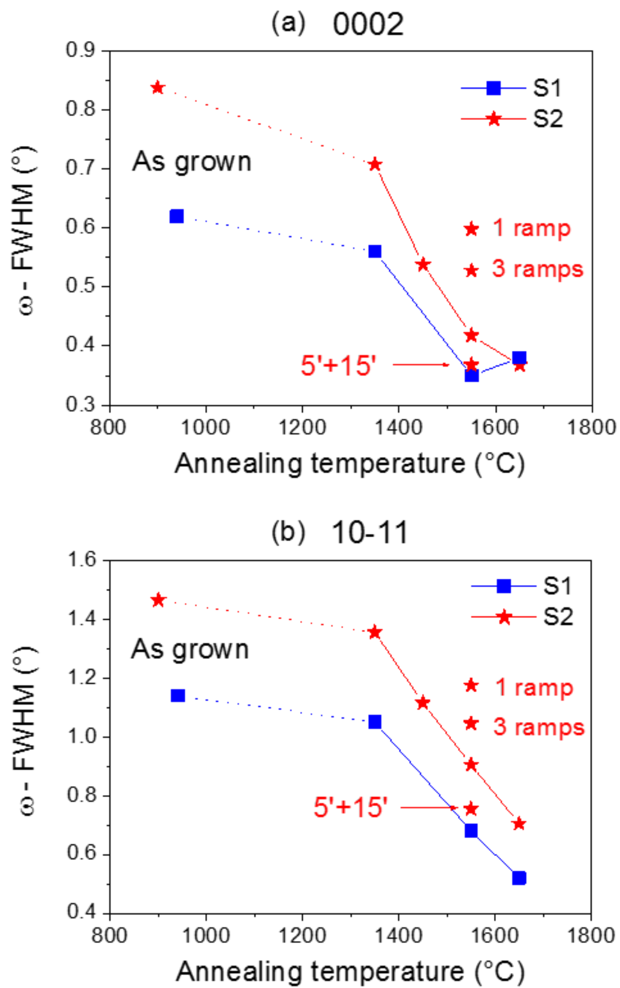

FIG. 1. Measured values of the ω-scan FWHM as a function of the annealing temperature for the (a) 0002 symmetric reflection and the (b) 10-11 skew reflection. The points at 940°C (S1) and 900°C (S2) correspond to the as-grown samples of AlN on sapphire.

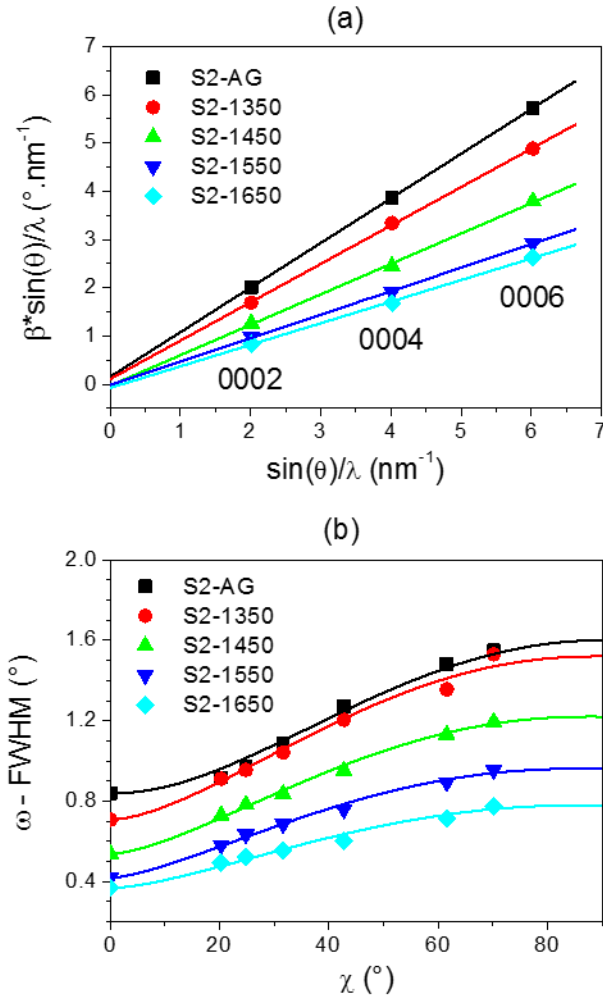

FIG. 2. (a) Williamson-Hall plots for symmetric reflections. β is the integral breadth of the ω-scan. The slopes of the different plots correspond to the tilt of the different samples (See Table I). (b) ω-scan FWHM of skew symmetric reflections vs inclination angle of the reflection measured from the 0002 reflection. Solid lines are fits to Srikant's model to determine the twist value of the samples (See Table I).

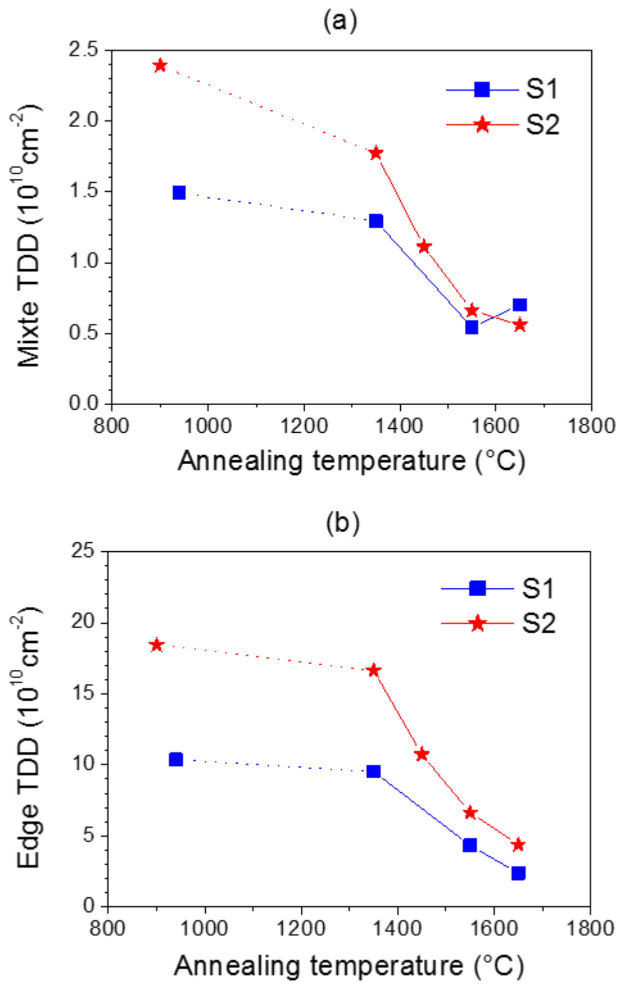

FIG. 3. (a) Mixed and (b) edge dislocation densities calculated from tilt and twist values vs the annealing temperature. The points at 940°C (S1) and 900°C (S2) correspond to the as-grown samples of AlN on sapphire.

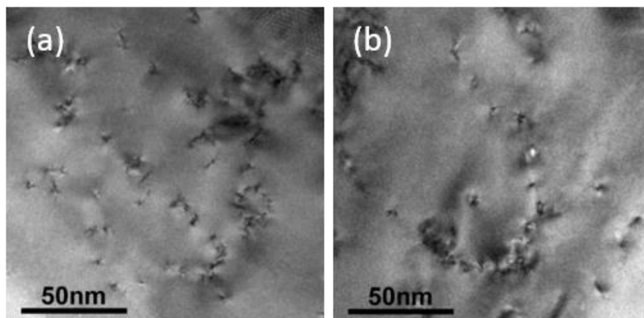

FIG. 4. TEM plane view images of (a) the S1 as-grown sample and (b) after the annealing at 1550°C for 5 min.

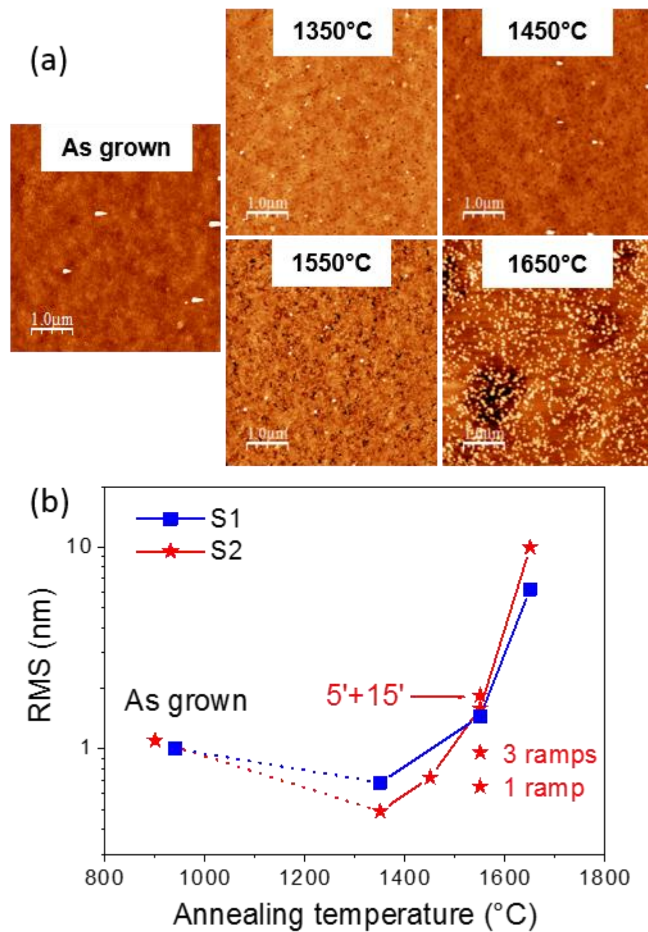

FIG. 5. (a) AFM images of S2 samples. (b) RMS of the AlN surface as a function of the annealing temperature. The points at 940°C (S1) and 900°C (S2) correspond to the as-grown samples.

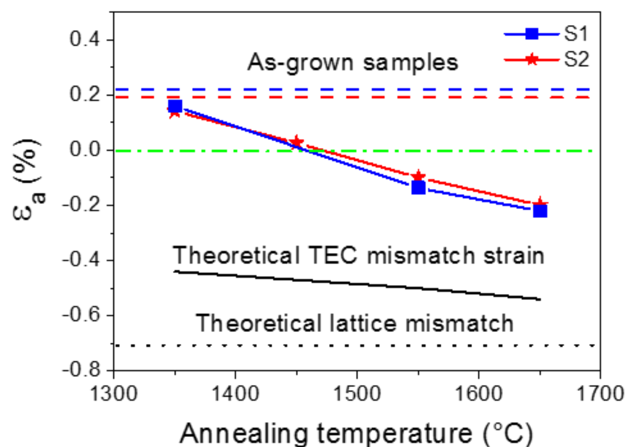

FIG. 6. In-plane strain of annealed AlN layers grown on sapphire vs the annealing temperature. The blue and red dashed horizontal lines correspond to the as-grown samples strain. The black horizontal dot line corresponds to the theoretical lattice mismatch and the black straight line corresponds to the theoretical thermal expansion coefficient mismatch strain.